GEOPHYSICS, VOL. 84, NO. 3 (MAY-JUNE 2019); P. F85–F95, 16 FIGS.
10.1190/GEO2018-0481.1

Particula: A simulator tool for computational rock physics of granular media

Mustafa A. Al Ibrahim[1], Abdulla Kerimov[2], Tapan Mukerji[3], and Gary Mavko[2]

ABSTRACT

Granular dynamics simulations provide insights to the contact-scale physics of loose sediments. However, simulations using identical spherical grains do not reflect characteristics observed in natural sediments, such as pack sorting, grading, grain sphericity, and grain roundness. We have developed software to create 3D grain packs of a range of regular and irregular shapes with geologically realistic variations in sorting and grading. An efficient approach is used to create multiple realizations of nonspherical irregularly shaped grains using coherent noise modification of the spherical grain surface. The discrete-element method is used to assemble the grain pack with different depositional styles by letting grains fall under the influence of gravity. Characterization of various parameters of random loose and dense grain packs, and comparison with previous studies, helps to establish the validity, flexibility, and consistency of the simulator. The output of this software is a digital grain pack, including metadata such as contacts and coordinates, that can be studied further using other analysis tools, e.g., by conducting fluid flow, mechanical, or electrical simulations.

INTRODUCTION

Studies on granular media are essential for understanding a wide range of physical phenomena in sediments including flow, stress and strain, heat conduction, and electrical effects. Granular media are ubiquitous and play an important role in industry, mining, and geophysics. Particularly in geophysics, the study of granular media is important because the physical properties of the grains and their arrangement, orientation, and size affect several processes and properties such as the (1) effective elastic moduli, which control seismic wave propagation (e.g., Paterson, 1956; Sain et al., 2016), (2) rock porosity and permeability, which control fluid flow (e.g., Yin and Nur, 1993; Diyokeugwu and Glover, 2018), and (3) electrical current transport, which controls effective electrical conductivity (e.g., Guo et al., 2018). For example, Sain et al. (2016) conclude that effective-medium theory models traditionally used in geophysics fail to predict the stress-dependent elastic properties of granular media because they do not account for the heterogeneous distribution of contacts and stress heterogeneity observed in simulated grain packs. Yin and Nur (1993), using experiments on unconsolidated clean Ottawa sand mixed with clay, find that permeability is affected by clay content weight percentage, whereas the percentage is less than a certain clay-content threshold, named critical clay-content. Guo et al. (2018) conclude from finite-element simulations that the effective permittivity of a rock responds differently to changes in pore-size variation, shape variation, distribution, and arrangement. The examples above use the physical experiments and numerical simulation, each with its own advantages and disadvantages.

Natural granular media are heterogeneous and pose a challenge for systematically isolating the effects of individual factors (e.g., sphericity, roughness, or sorting) on the physical properties of the granular media. To overcome these limitations, physical experiments using synthetic grain packs have also been used in the past (e.g., Bernal, 1959, Scott, 1962; Finney, 1970; Fu and Dekelbab, 2003; Knackstedt et al., 2009). Rare data sets are available to the scientific community such as the Finney (1970) pack. Although the results are very useful, conducting such experiments to generate realistic grain pack is time consuming and expensive. In addition, incorporating different grain shapes in a systematic manner is difficult.

Numerical discrete element simulation has been a very useful tool to study granular media. Most often numerical simulations work with

Peer-reviewed code related to this article can be found at http://software.seg.org/2019/0006.
Manuscript received by the Editor 3 July 2018; revised manuscript received 26 November 2018; published ahead of production 07 February 2019; published online 10 April 2019.
[1]Stanford University, Energy Resources Engineering Department, Stanford, California, USA. E-mail: malibrah@stanford.edu.
[2]Stanford University, Geophysics Department, Stanford, California, USA. E-mail: akerimov@stanford.edu; mavko@stanford.edu.
[3]Stanford University, Energy Resources Engineering Department, Stanford, California, USA and Stanford University, Geophysics Department, Stanford, California, USA. E-mail: mukerji@stanford.edu.

spherical or other regular grain shapes. Extensions to irregular natural grain shapes can be computationally challenging. As described later, one of the challenges is to keep track of contacts for irregular grain shapes. However, with advances in contact simulation theory, computer science, and hardware acceleration, numerical simulations can now be used to generate a range of digital grain packs efficiently. This is done by modeling the granular media as a random packing of discrete grains, most commonly spheres. These grain packs have specific characteristics that can be systemically studied, such as void fraction or porosity, permeability, and pore body and throat-size distributions.

We introduce software for generating 3D grain packs. The software is flexible enough to generate a variety of grain packs with different grain shapes, grain-size distributions, and grading. To accomplish this, we introduce an efficient numerical approach to create nonspherical irregularly shaped grains using the coherent noise modification of an underlying regularly shaped grain surface. The various granular packs of grains with prescribed shape and size distributions are modeled and compared with numerical and experimental measurements. The approach outlined (1) satisfies the dynamic stability constraint under gravity, (2) has the ability to handle grain-size distributions, (3) creates regular and irregularly shaped grains, (4) allows for multiple grain types at the same time, (5) deposits grains using multiple scenarios (e.g., random, fining upward, coarsening upward), and (6) has the ability to create loose and dense packs.

In this paper, we first present the relevant previous work. Next, we summarize the discrete-element method framework used. Afterward, we introduce the new method to generate nonspherical grains and the workflow to produce the grain packs. Finally, we validate the workflow by showing some examples of generated grain packs and studying their corresponding characteristics. The output of this method can be used as an input for other simulations and studies, such as in flow, stress, and wave-propagation studies (García et al., 2004; García and Medina, 2006; Sain, 2010; Sain et al., 2014; O'Donovan et al., 2016). An example of using this software for studying the influence of irregular shape and size on porosity, permeability, and elastic properties of granular media is found in Kerimov et al. (2018).

BACKGROUND INFORMATION

Numerical simulation of granular media

Numerical simulations of granular media can be categorized broadly into two types: geometric and dynamic. Geometric methods, which rely on a set of relatively simple geometric rules, can quickly assemble packs of large number of grains (Jerier et al., 2010). For example, Jodrey and Tory (1985) simulate a monodisperse spherical pack from a random distribution of sphere centers by converging to a solution that eliminates overlap while minimizing the outer diameter of the pack. In a ballistic deposition algorithm (Aparicio and Cocks, 1995; Jullien and Meakin, 2000; Nurkanov et al., 2001), the spheres are added one by one in a geometrically stable position at the surface of an evenly packed set of spheres. The primary advantage of geometric methods is reduced computational time; a grain pack of 10,000 spherical grains can be created in a few minutes (Jerier et al., 2010). However, these geometrically generated numerical grain packs are commonly mechanically unstable and have no information on the contact forces between the grains in contact (Jerier et al., 2010).

Dynamic methods, based on the discrete element method (DEM) (Cundall and Strack, 1979), are used to computationally assemble packs of grains based on physical forces. They are commonly used to study concretes (Magnier and Donzé, 1998; Camborde et al., 2000; Monteiro Azevedo et al., 2008), ceramics (Tan et al., 2009), powders (Martin et al., 2003; Martin, 2004), and soils (Richefeu et al., 2006; Donzé et al., 2009; Sain, 2010). These dynamic methods can reproduce the grain-pack properties (Liu and Yuan, 2000; Yang et al., 2000), but are computationally more expensive than geometric methods. Different dynamic methods have been published. For example, Liu and Yuan (2000) and Sain (2010) generate grain packs based on an isotropic compression method, where nonoverlapping spheres are positioned and compressed to the prescribed stress. Lubachevsky and Stillinger (1990), Stillinger and Lubachevsky (1993), and Kansal et al. (2002) use an iterative growth algorithm to grow spheres and disks from an initial random configuration and grain velocities. Donev et al. (2005a, 2005b) and Bannerman et al. (2011) use the event-driven molecular-dynamics approach that is based on the simulation of series of grain collisions (events) by predicting their occurrence in the future from current grains trajectories. This event-based approach can be computationally efficient because time stepping is discontinuous between and during events.

Grain shapes

Many published studied related to 3D DEM modeling of granular media are based on spherical grains, which makes the contact detection and force calculation relatively easy compared with any other shape (e.g., Liu and Yuan, 2000; Fu and Dekelbab, 2003; Jiang et al., 2003; Bagi, 2005). Jin et al. (2003) use DEM to numerically generate grain packs of spherical grains with a prescribed grain-size distribution and model the effect of compaction by applying a vertical stress and allowing overlap of the spherical grains. The random loose and dense monodisperse sphere grain packs have been extensively studied in experiments and simulations, which typically have a maximal porosity of approximately 0.40 (Dullien, 1991) and 0.36 (Baule and Makse, 2014), respectively. However, grains with irregular shapes are ubiquitous in nature and in many industries involved in granular processing. Theoretical or numerical modeling of grain packs with nonspherical grains is a difficult problem due to the shape, position, and orientation of these grains (Baule and Makse, 2014). Recent works have focused on grain packs of nonspherical regularly shaped grains, such as ellipsoids (Lin and Ng, 1997; Mustoe and Miyata, 2001), disks (Stillinger and Lubachevsky, 1993), tetrahedrons (Zhao et al., 2015), and polyhedrons (Hart et al., 1988; Abou-Chakra et al., 2004). There is still a need for rigorous simulation and analysis of grain packs consisting of nonspherical irregularly shaped grains because studies have shown that the grain packs' physical properties, such as porosity, permeability, and the elastic bulk modulus are dependent on the morphological characteristics of the constituent grains (Latham and Munjiza, 2004; Kerimov et al., 2018).

A popular approach to approximate irregular grain shapes is to use multispheres. The approach is based on clumps, clusters, or clouds of overlapping or nonoverlapping small spheres to represent the large nonspherical irregular shape grain, in which internal contacts are ignored and the cluster behaves as a rigid body (Matsushima et al., 2003; Price et al., 2007; Wang et al., 2007; García et al., 2009; Gao et al., 2012). Matsushima et al. (2003) fill the volume of a nonspherical grain with a cluster of overlapping spheres. Their method randomly generates small spheres of different sizes inside the nonspherical grain volume. The spheres are then optimized by moving and expanding or shrinking the small spheres using virtual forces to make them fit optimally within the boundaries of the non-

spherical grain. Unfortunately, the convergence criterion of this problem significantly depends on initial random locations of the small overlapping spheres and virtual force magnitude. Price et al. (2007) also use small spheres to optimally fit the volume of nonspherical grains. They fill the volume of the nonspherical grain by repeatedly generating a sphere through four random points chosen on the surface of the grain. The process is optimized by expanding or shrinking the spheres via local minimization of the distance between the spheres and the surface of the nonspherical grain. The optimization technique is extremely efficient when the four random points were selected locally in the same area of the grain. The optimization and grain assembly make the approach computationally expensive and not easily applicable to numerical grain packs of large number of grains with different shapes and sizes. Wang et al. (2007) propose a clustering approach in which the volume of the nonspherical grain is filled with a regular structural arrangement of small nonoverlapping spherical grains, followed by replacing the agglomerate of adjacent small spherical grains with a large one to reduce the computational time. The main disadvantage of this approach is that the rough surface of the produced nonspherical grain that might be not representative of the surface of granular grains. García et al. (2009) incorporate overlapping spheres to achieve an acceptable representation of irregular grains using minimum number of spheres.

Other approaches for generating irregular grain packs exist that are not based on the multisphere. For example, Latham et al. (2001) simulate loose packs of tetrahedra by a random positioning step followed by an overlap removal step. Latham and Munjiza (2004) compare cube-packing experiments with simulation results obtained using the finite-element method and DEM. Lee et al. (2009) represent grains as a set of intersecting half-spaces to create polyhedrons. Tahmasebi et al. (2017), Tahmasebi and Sahimi (2018), and Tahmasebi (2018) use an image-based Markov process to construct different realizations of granular media from X-ray scanned grains.

NUMERICAL METHOD AND PROCEDURES

In this section, we provide (1) a general description of the DEM method used in this study, (2) a new efficient numerical approach to create nonspherical irregularly shaped grains using coherent noise modification of the spherical grain surface, and (3) the workflow to assemble 3D loose and dense grain packs.

Numerical framework

The DEM is a powerful method to simulate the interactions between discrete objects (Cundall and Strack, 1979; Pöschel and Schwager, 2005), including irregularly shaped (Matuttis and Chen, 2014) objects. DEM methods model the individual grain collisions, where each grain collision must satisfy the conservation laws for linear and angular momentum. There are three essential elements in DEM: contact detection, contact resolution, and time-step integration. In this study, the PhysX solver is used, which is implemented in the Unity3D development platform (Unity Technologies, 2017), to simulate grain packs with spherical and nonspherical shapes under the influence of gravitational forces. The PhysX solver was created for real-time physics calculations; therefore, there is a trade-off between computational efficiency, flexibility, and accuracy (Messmer, 2014). In particular, the current solver is not accurate when dealing with fast angular velocities, or collisions with very high mass ratios if a small number of solver iterations is used (Storey et al., 2018). Other solvers prefer accuracy over efficiency and flexibility, such as LIGGHTS (Kloss et al., 2012) and ChronoEngine (Tasora and Negrut, 2016). Advantages of real-time physics solvers are being recognized in the scientific community and are being used for specific scenarios related to earth science that demand efficiency over extreme accuracy (e.g., Longshaw et al., 2010; Longshaw, 2011). For natural sediments, we often have to simulate multiple grain packs with stochastic variations to draw meaningful statistical correlations. For such applications, real-time physics solvers are very efficient.

Contact detection

The collision is handled in two phases: (1) broad-phase and (2) narrow-phase. Broad-phase collision detection approximates the shape of the grains by its referential axis-aligned bounding box and detects overlapping boxes. The implemented algorithms used to do this are sweep and prune and multibox pruning (based on Terdiman, 2001). The narrow-phase collision detection algorithm is only applied on object pairs that were detected in the broad phase. In this phase, the exact point contacts are identified as well as the penetration depth. Parallelization of the problem by grouping different grains, a.k.a. island generation, is another modification that is implemented to decrease the processing time (Tonge et al., 2012). The grouping introduces a slightly nondeterministic solution because the grouping might be different depending on the number of grains in the simulation (Storey, 2017). To improve collision detection of fast-moving objects, continuous collision detection attempts to predict the possible collisions before they occur and informs the numerical integrator.

Contact resolution

PhysX uses an impulse-based solver (e.g., Hahn, 1988; Mirtich, 1996). Figure 1 shows the general procedures to update a grain's position and velocity based on an external impulse. The velocity is calculated along the contact normal. The impulse is calculated such that the relative velocity is zero and then converted into the rigid body coordinates. The calculated impulse is then applied to the rigid body velocity, and the position is updated using this velocity.

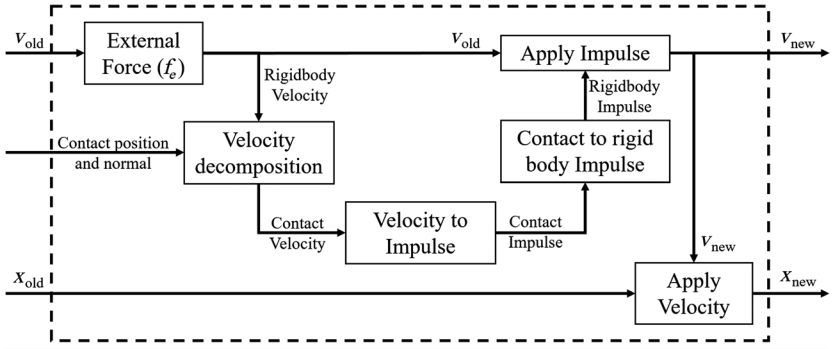

Figure 1. Schematic of grain velocity and position update subjected to external forces (modified after Tonge, 2012).

The rigid body contact model and discretization used have been described in Anitescu and Potra (1997) as well as Tonge et al. (2012). A brief summary is provided here. Consider n rigid bodies with positions/rotation $\bar{\mathbf{x}} \in \mathbb{R}^{6n}$, external forces (such as gravity) and torques $\bar{\mathbf{f}}_e \in \mathbb{R}^{6n}$, and masses/rotation inertia $\bar{\bar{\mathbf{M}}} \in \mathbb{R}^{6n\times 6n}$. The collision detection identifies the m contacts between rigid bodies, represented by contact constraints $\phi(\mathbf{x}) \geq 0$, where $\phi(\mathbf{x})$ is a continuous differentiable function of the position vector. The Jacobian ($\bar{\bar{\mathbf{J}}} \in \mathbb{R}^{m\times 6n}$) is thus defined as $\partial\phi/\partial\mathbf{x}$. The fundamental equation solved in the system is Newton's second law of motion (equation 1) under the Signorini condition, where the impulse ($\bar{\lambda} \in \mathbb{R}^m$) is defined as the change in momentum. The number of unknowns and equations is six per grain. The velocity ($\bar{\mathbf{v}} \in \mathbb{R}^{6n}$) Signorini conditions (Tonge et al., 2012) state that the impulses must be positive (i.e., $\bar{\lambda} \geq 0$), velocities must remove any system penetrations (i.e., $\bar{\bar{\mathbf{J}}}\,\bar{\mathbf{v}} \geq 0$), and impulses are only applied at contacts if the contacts are not separated ($\bar{\lambda} \geq 0$ and $\bar{\bar{\mathbf{J}}}\,\bar{\mathbf{v}} \geq 0$):

$$\bar{\bar{\mathbf{M}}}\,\ddot{\bar{\mathbf{x}}} = \bar{\bar{\mathbf{J}}}^{\mathbf{T}}\bar{\lambda} + \bar{\mathbf{f}}_e. \tag{1}$$

Equation 1 can be discretized using a semiimplicit stepping scheme with time step h to produce equation 2

$$\bar{\bar{\mathbf{M}}}(\bar{\mathbf{v}}_{\mathbf{new}} - \bar{\mathbf{v}}_{\mathbf{old}}) = h\bar{\bar{\mathbf{J}}}^{\mathbf{T}}\bar{\lambda} + h\bar{\mathbf{f}}_e. \tag{2}$$

The Signorini conditions causes the discretized equation to be solved as a linear complementary problem (LCP) (Anitescu and Potra, 1997; Tonge et al., 2012), as described in equations 3–5 to obtain the unknown impulses ($\bar{\lambda}$), which contain m unknowns

$$\bar{\mathbf{q}} = \bar{\bar{\mathbf{J}}}(\bar{\mathbf{v}}_{\mathbf{old}} + h\bar{\bar{\mathbf{M}}}^{-1}\bar{\mathbf{f}}_e), \tag{3}$$

$$\bar{\bar{\mathbf{N}}} = \bar{\bar{\mathbf{J}}}\,\bar{\bar{\mathbf{M}}}^{-1}\bar{\bar{\mathbf{J}}}^{\mathbf{T}}, \tag{4}$$

$$\bar{\lambda} = \mathrm{LCP}(\bar{\bar{\mathbf{N}}}, \bar{\mathbf{q}}). \tag{5}$$

The updated new velocity ($\bar{\mathbf{v}}_{\mathbf{new}}$) and position ($\bar{\mathbf{x}}_{\mathbf{new}}$) can be calculated using equations 6 and 7:

$$\bar{\mathbf{v}}_{\mathbf{new}} = \bar{\mathbf{v}}_{\mathbf{old}} + h\bar{\bar{\mathbf{M}}}^{-1}\bar{\bar{\mathbf{J}}}^{\mathbf{T}}\bar{\lambda} + h\bar{\bar{\mathbf{M}}}^{-1}\bar{\mathbf{f}}_e, \tag{6}$$

$$\bar{\mathbf{x}}_{\mathbf{new}} = \bar{\mathbf{x}}_{\mathbf{old}} + h\bar{\mathbf{x}}_{\mathbf{new}}. \tag{7}$$

Friction is implemented using an approximation to the Coulomb friction model (Tasora et al., 2008; Tonge et al., 2012). With friction, the LCP is substituted with a boxed LCP. The model assumes that the tangential force and tangential velocity are opposite in direction. It is solved at each contact point (a friction force is calculated at each contact point). Because the model is based on a point-force calculation, it is not suitable for cases in which there is a very large number of contact points between two objects, e.g., when the contact is a surface.

The coefficient of restitution ($0 \leq \mathrm{COR} \leq 1$) is defined as the ratio of relative velocities after and before collision, and it accounts for the loss of kinetic energy during each collision. It is used to account for the inelastic collisions of the grains.

Time-step integration

Because a granular system typically contains a multitude of individual grains, direct integration of the system can be computationally expensive. The implementation of integrator and collision detection algorithms of DEM requires some care to keep the system numerically stable. An unstable integrator will lead to jittering of grains, which forces the use of very small time steps making it

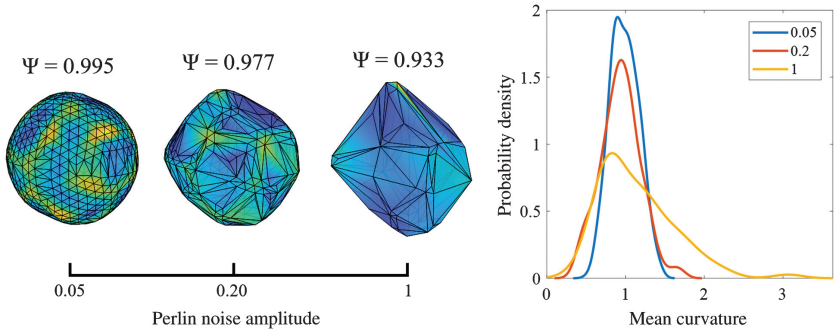

Figure 3. Three nonspherical irregularly shaped grains are generated using different Perlin noise amplitudes based on the numerical procedures described in the text and outlined in Figure 2. All three nonspherical grains have × same volume. The corresponding mean curvature distributions and average sphericity index are calculated. The Perlin noise frequency is 3, × octave count is 3, lacunarity is 0.5, and persistence is 0.5.

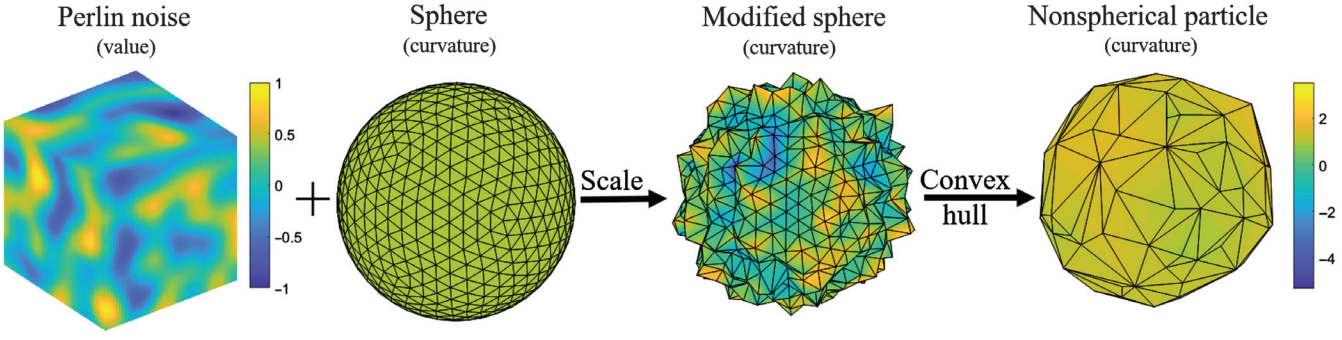

Figure 2. A procedure for creating a nonspherical irregular-shape grain. The Perlin noise cube is colored by its values; the sphere, modified sphere, and nonspherical grain are colored by the value of the mean curvature.

computationally expensive. PhysX uses an iterative scheme to solve the conservation of momentum equations on multiple contacts (Tonge, 2012; Tonge et al., 2012). This is done by sequentially solving contact pairs at the time step and looping through the procedure multiple times until the solution is converged (Tonge, 2012). The number of iterations required is typically less than 10 to obtain reasonable results for rendering purposes. Using a stable integrator allows for using a large time step without losing accuracy. A semi-implicit Euler integrator is used, which guarantees convergence as opposed to an explicit scheme, which is conditionally convergent (Gavrea et al., 2008).

From spherical to nonspherical grain shapes

In this section, we describe how we create irregularly shaped grains. Correlated noise is used here to generate multiple realizations of nonspherical irregular grain shapes. Figure 2 illustrates the numerical procedure for creating a nonspherical irregular grain. The procedure consists of the following steps: (1) generating a spherical mesh using the regular convex icosahedron approximation (Popko, 2012), (2) generating 3D coherent noise cube, (3) displacing the spherical mesh by adding the values of the scaled 3D coherent noise at spherical mesh vertices, (4) computing the convex hull of the result (Barber et al., 1995), and (5) scaling the nonspherical grain based on the given volume or the radius of the spherical grain.

In this study, we used 3D Perlin noise to modify the spherical meshes (Perlin, 1985, 2002). Perlin noise is a type of gradient noise that produces correlated noise (Figure 2). The noise is generated by interpolating between gridded pseudorandom basis gradient vectors. To speed up the calculation, the basis vectors can be sampled from a small set of vectors that have special characteristics, such as their simplistic dot-product calculation (Perlin, 2002). The interpolation between the gradients is commonly calculated using a fifth-degree polynomial to ensure continuous first and second derivatives of the resultant noise. Multiscale noise is incorporated into the algorithm by superimposing different Perlin noise functions at multiple frequency (wavenumber) bands with higher frequencies having lower amplitudes. The parameters used in the Perlin noise implementation are the number of octaves; the frequency; the lacunarity, which measures the decrease in frequency per octave; the persistence, which measures the decrease in amplitude per octave; and an overall amplitude factor.

In this study, the Perlin noise amplitude factor is varied to produce grains with different morphological aspects. Because Perlin noise is stochastic, multiple unique realizations of the grains can be generated. Figure 3 illustrates three generated nonspherical irregularly shaped grains using different Perlin noise amplitudes based on the procedure described in Figure 2. All three nonspherical grains have the same volume. We quantify the shape of

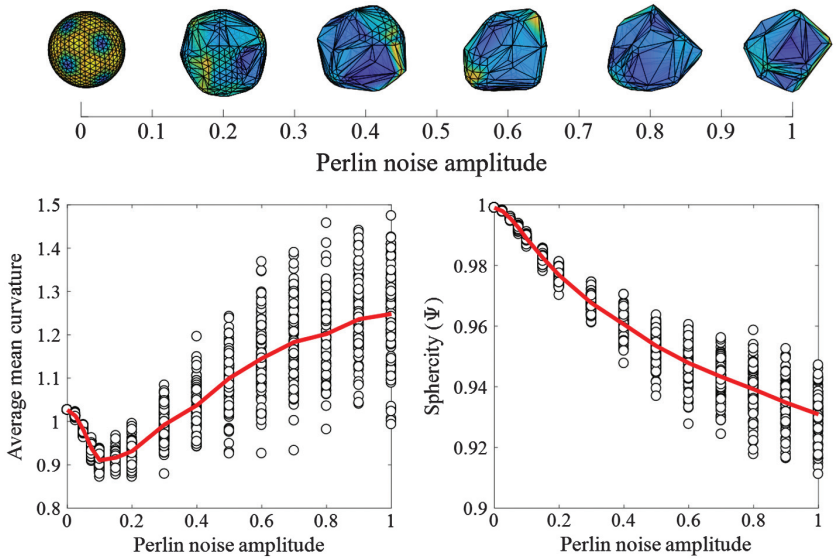

Figure 4. Mean of mean curvature and sphericity as a function of the Perlin noise amplitude (bottom). Grains corresponding to the mean values are also illustrated (top). Coloring is based on the curvature values for the grain. The Perlin noise frequency is 3, the octave count is 3, lacunarity is 0.5, and persistence is 0.5.

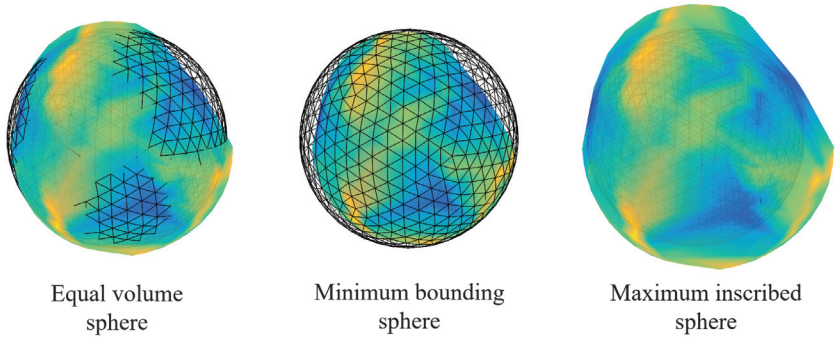

Figure 5. Three different approaches are implemented to compute the size of the nonspherical irregularly shaped grain by relating to a given size of spherical grain.

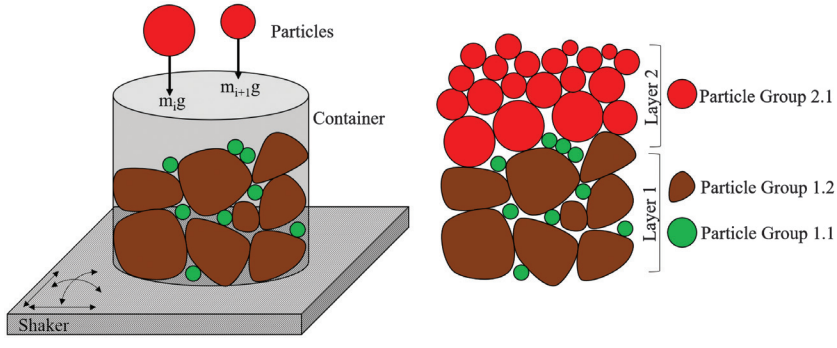

Figure 6. Schematic architecture of the 3D grain pack with prescribed grain shape and size distributions.

the nonspherical grain using the grain surface mean curvature and the sphericity. Gatzke and Grimm (2006) provide a review of the methods available for estimating curvature on triangular meshes. The mean curvature H is defined as the average of the two principal, maximum and minimum, curvature values. Additionally, the sphericity Ψ (Wadell, 1935) is defined as the ratio between the surface area of a sphere with the same volume as the given grain to the surface area of the grain (equation 8), where V_p is the volume of the grain and A_p is the surface area of the grain:

$$\Psi = \frac{\pi^{\frac{1}{3}}(6V_p)^{\frac{2}{3}}}{A_p}. \quad (8)$$

The sphericity of a sphere is equal to 1.0, whereas the sphericity of nonspherical grains is less than 1.0. Figure 3 shows the corresponding mean-curvature distributions and average sphericity index calculated for three nonspherical grains. Figure 4 shows the mean of the mean curvature and sphericity as a function of the Perlin noise amplitude. The average mean curvature generally decreases for low noise values and increases afterward. The sphericity, on the other hand, always decreases with the increasing amplitude. The exact relationship with respect to the amplitude depends on the other parameters used in the Perlin noise implementation, i.e., frequency, octave count, lacunarity, and persistence.

The size of the nonspherical irregularly shaped grains can be calculated in several ways by relating to a given spherical grain size as depicted in Figure 5. Three different approaches are implemented: (1) by equating the volume of the grain to the volume of the sphere, (2) by inscribing the grain in the sphere (Fischer et al., 2003), or (3) by inscribing the sphere in the grain. Note that option (1) preserves the volumetric input distribution. More complex shapes and processes can also be integrated. Grains, such as shells, can be generated using previously defined shapes using external modeling software or generated procedurally in real time (if they can be parameterized). A current limitation is set on the number of vertices in the mesh; therefore, external software might be needed to resample high-resolution meshes to lower resolution such as the free and open source MeshLab (Cignoni et al., 2008).

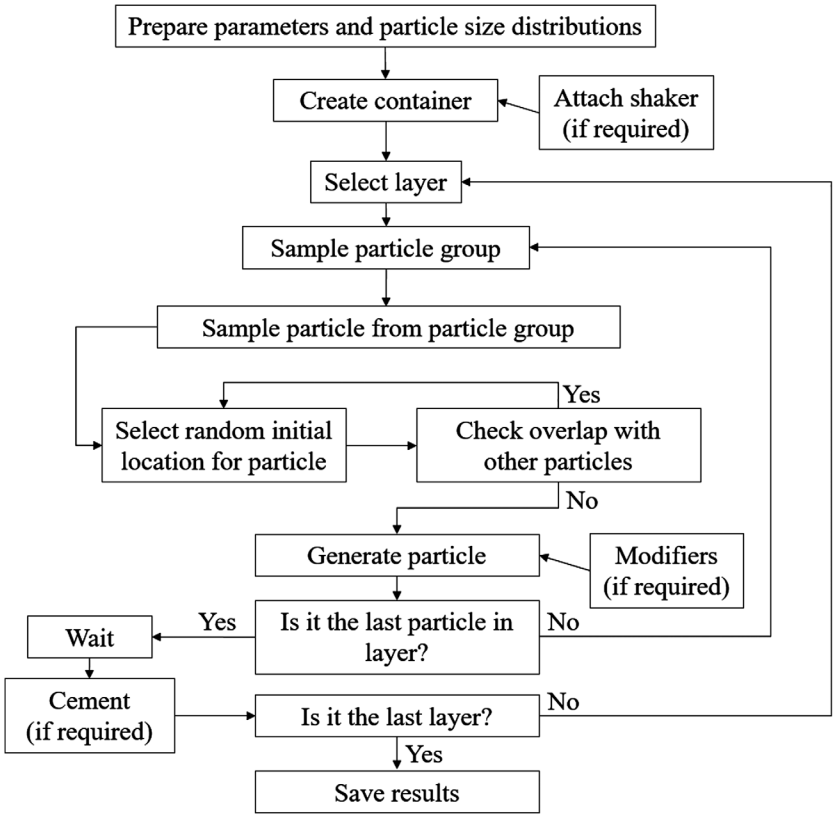

Figure 7. A general workflow to generate grain packs of spherical and nonspherical grains.

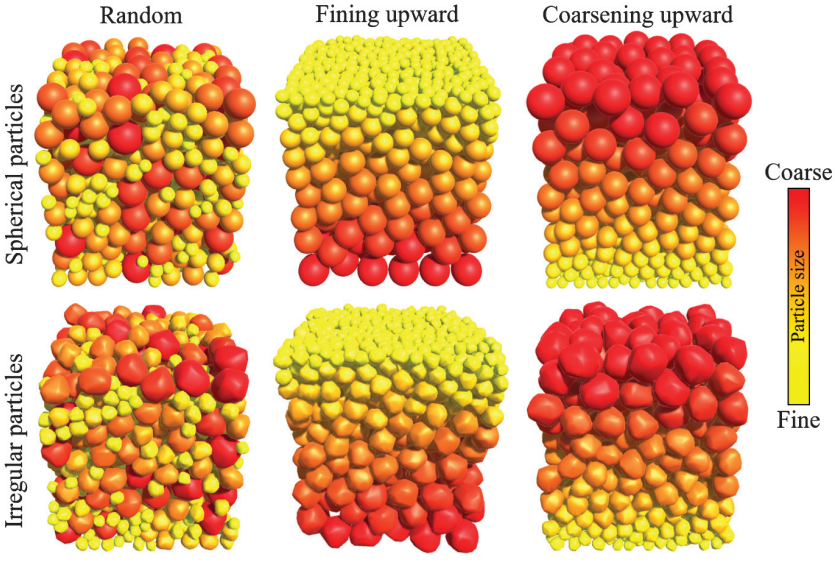

Figure 8. Simulations of random, fining upward, and coarsening upward grain packs of spherical and nonspherical irregularly shaped grains.

Assembling of grain packs

The grain pack is assembled by pouring grains with prescribed grain-size distribution in a container under the influence of gravitational force (Figure 6). A grain pack is made of layers deposited sequentially. Each layer is composed of grain groups that are deposited simultaneously, and each grain group is made of several grains. Each grain group has a specified shape, properties (such as density, friction, and coefficient of restitution), and prescribed grain-size distribution. The shapes of the grains can be defined as spherical, nonspherical regular (cubes, cylinders, ellipsoids, etc.), and nonspherical irregular. The

total number of grains in the simulation is defined by the user. The proportion of the various grain groups and layers can be defined based on volume or frequency.

The practical workflow to assemble the grain pack is depicted in Figure 7. A virtual container (a rectangular box or a cylinder) is used to collect the generated grains. The size of the container can be set manually or estimated automatically from the expected total grain volume and the expected pore fraction in the resultant grain pack. Given a layer with one or more grain groups, random sampling based on the proportion of each grain group is used to determine the next grain type. The grain is then generated based on either random sampling from the size distribution, fining upward rule, or coarsening upward rule (Figure 8). A possible random position in the x-y plane above the container is sampled and tested for overlap with previously generated grains. If there is an overlap, a new random position is sampled. If there is not an overlap, the grain is created at that position and allowed to freely fall under the influence of gravity. Once a layer is deposited, a user-defined rest period is used to make sure that the layer comes to rest. The layer can also be cemented if desired, i.e., the grains are constrained into their position with no rotation, after the rest period. The next layer is then deposited as defined. Once assembling is finished, outputs can be saved. A data file is exported that contains the final location, rotation, scale, and volume of each grain. Mesh files of the grain pack and each grain separately can be exported for further analysis.

Note that the approach described above produces poured loose grain packs. Shaking is implemented to attempt to simulate poured dense grain packs by vibrating the container as depicted in Figure 6. There are two types of shaking methods: translational and rotational shaking. Translation shaking (dx) was done using a random translation in the three dimensions (equation 9), where $\max(p)$ is the

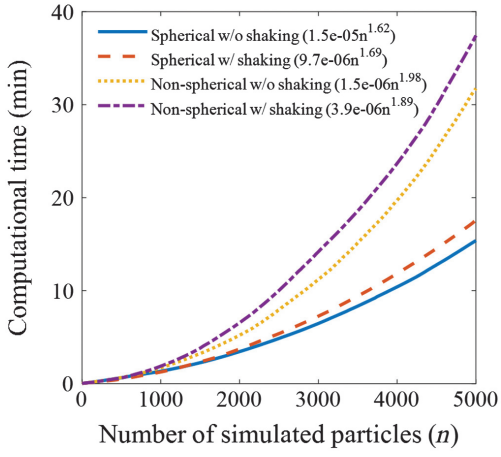

Figure 9. Computational time as a function of grain number n. The computer specifications used are listed in the text.

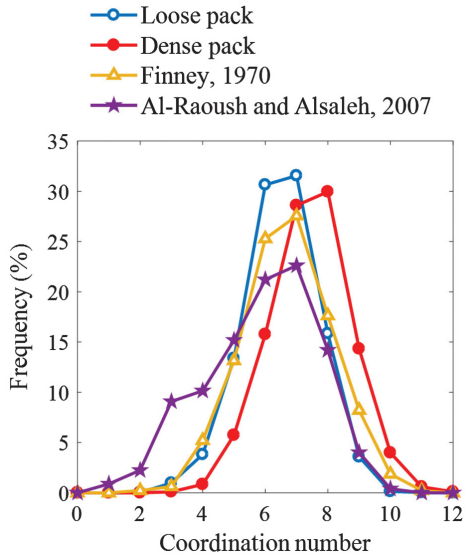

Figure 11. Comparison of coordination number distributions computed from the simulations of random loose and dense grain packs of identical frictionless spherical grains with data from Finney (1970) and Al-Raoush and Alsaleh (2007).

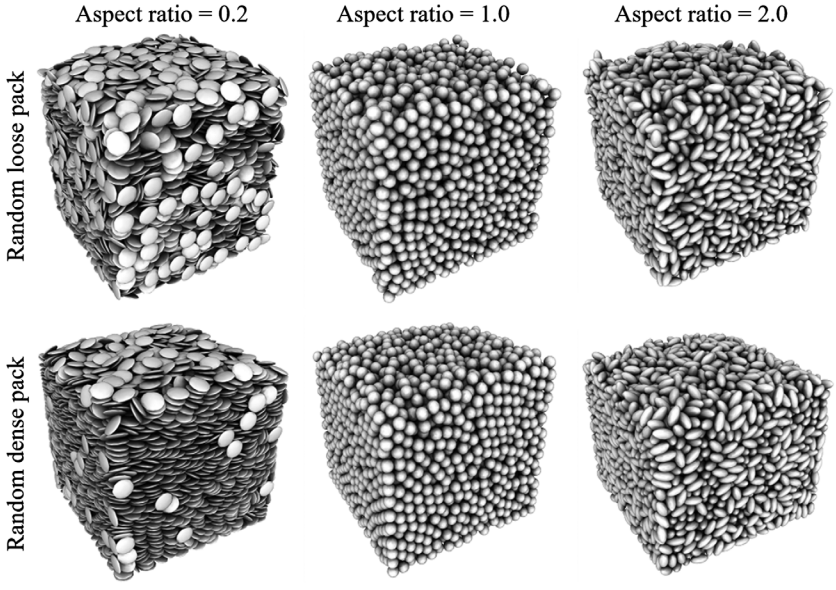

Figure 10. Random loose and dense monodisperse grain packs of 5000 ellipsoids with aspect ratios of 0.2 (i.e., disks), 1.0 (i.e., sphere), and 2.0 (i.e., needles).

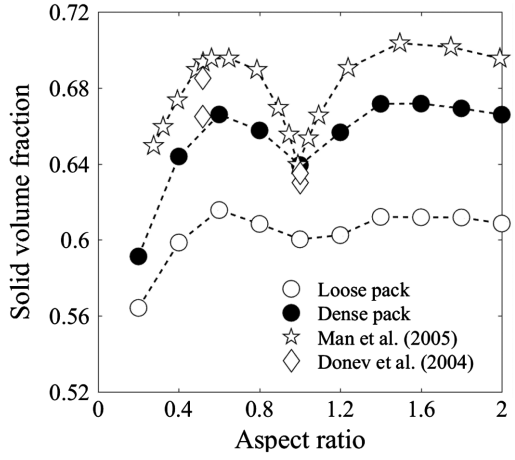

Figure 12. Comparison of solid volume fractions computed from the simulations of random loose and dense grain packs of frictionless ellipsoids with various aspect ratios between 0.2 and 2.0 with Man et al. (2005) and Donev et al. (2004) data.

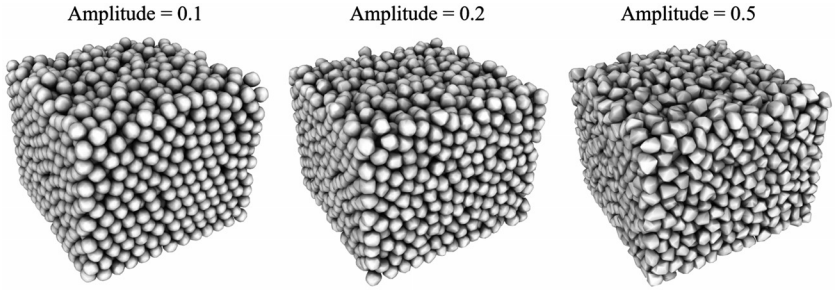

Figure 13. Random dense monodisperse grain packs of 2500 nonspherical irregular shape grains with Perlin noise amplitudes of 0.1, 0.2, and 0.5.

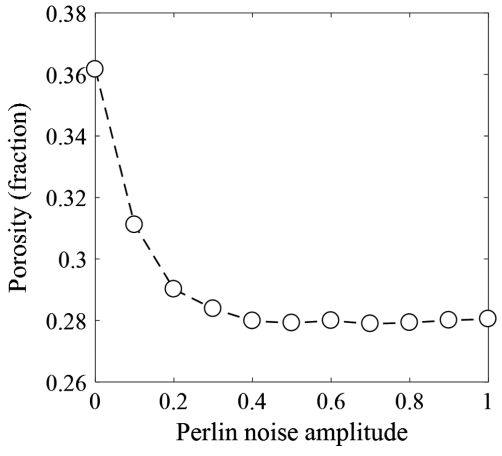

Figure 14. The computed porosity of random dense monodisperse grain packs of nonspherical irregularly shaped grains as a function of Perlin noise amplitude. Note that the zero Perlin noise amplitude corresponds to random dense monodisperse grain pack made up spherical grain, which typically have a porosity of approximately 0.36 (Baule and Makse, 2014).

maximum translation measured as a percentage of the container length in each direction. Rotational shaking ($d\phi$) is done by random rotation (equation 10) around the bottom center of the container with $\max(\phi)$ being the maximum rotational angle. The magnitude of the shaking can be defined by the user. In addition, pressure can be applied using the container lid to create a more dense grain pack.

$$dx = \text{random range}(0, 1) \times \max(p), \tag{9}$$

$$d\phi = \text{random range}(0, 1) \times \max(\phi). \tag{10}$$

The computational time for each grain pack is in the order of tens of minutes. Figure 9 shows the benchmark results using a 2013 iMac with a 3.5 GHz Intel i7 processor, a 16 GB 1600 MHz DDR3 RAM, and an Nvidia GeForce GTX 775M graphic card. Computational time can be modeled by a power law with an exponent of approximately 1.6–1.7 for spherical grains and approximately 1.9–2.0 for irregularly shaped grains. As expected, shaking the container increases simulation time as more grains are moving and more contacts are involved in the simulation.

Characterization of the grain packs

In this section, we present and characterize the structure of the generated random loose and dense assemblies of spherical, nonspherical regular (ellipsoids with various aspect ratio), and nonspherical irregular grains. To characterize the grain shape, the sphericity and mean curvature definitions are used. Additionally, we compared the porosity estimates obtained from the simulations with published numerical and experimental measurements in the literature.

Spherical and nonspherical regular shapes

We generated two sets of grain packs with 10 different random monodisperse frictionless ellipsoids (each with 5000 grains) with aspect ratios between 0.2 and 2.0 (e.g., Figure 10). The first grain pack set is a random loose pack. The second set is a random dense pack, which is achieved by continuously shaking the container with translational and rotational shaking maximum magnitudes of $0.0002 \times D_{\text{container}}$. This magnitude of translational and rotational shaking is chosen to attempt to generate random dense grain pack of identical spheres, which typically have a porosity of approximately 0.36 (Baule and Makse, 2014). All of the grains have the same density of 2.65 g/cm^3, that of a quartz mineral. The static and dynamic coefficients of friction between individual grains are assumed to be zero; in other words, the grains are frictionless. The coefficient of restitution is assumed to be 0.1 to prevent continuous elastic bounciness of the grains in the container.

In Figure 11, we compared the coordination number distributions computed from the simulations of random loose and dense grain packs of identical frictionless spherical grains with analysis applied on the Finney (1970) grain pack and the analysis of Al-Raoush and Alsaleh (2007). The coordination number distribution from the generated random loose grain pack is consistent with other

experimental studies of glass beads. Note that Al-Raoush and Alsaleh (2007) find that coordination number of less than four has a higher proportion than the generated grain pack and Finney (1970) grain pack. This could be due to the fact that Al-Raoush and Alsaleh (2007) include grains on the boundary of the experiment. This study and the results from the Finney grain pack do not include grains from the boundary. The generated dense pack shifts the coordination number distribution to higher values, as expected.

Additionally, we computed the solid volume fraction as a function of the grain aspect ratio (Figure 12). The results are consistent with the simulation results from Man et al. (2005), which state that some random dense grain packs of ellipsoids with prescribed aspect ratio are as dense or denser than random dense grain pack of spheres, as depicted in Figure 12. The porosity, approximately 0.36, of the random dense grain pack of the spheres, is in good agreement with Man et al. (2005); however, the porosity values of the random dense grain pack of ellipsoids with varying aspect ratios are higher than the ones in Man et al. (2005). The discrepancy can be explained by the fact that Man et al. (2005) simulate the grain packs under confining pressure, which will result in lower porosity. Donev et al. (2004) conduct lab experiments on oblate spheroids with aspect ratios of approximately 0.52 and 0.53, where the measured solid volume fractions are approximately 0.665 and 0.695, respectively. These experimental results fall between our and Man et al.'s. (2005) numerical results.

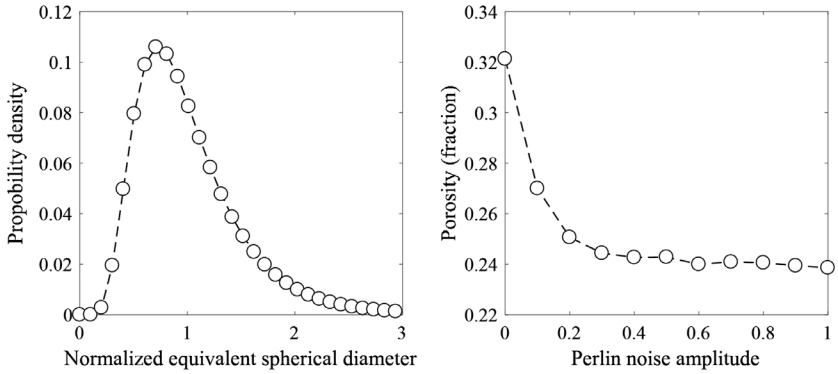

Figure 16. (a) Log-normal nonspherical irregular grain-size distribution in a random dense polydisperse pack and (b) computed porosity of random dense polydisperse grain packs of nonspherical irregularly shaped grains as a function of the Perlin noise amplitude. Note that the zero Perlin noise amplitude corresponds to a random dense polydisperse grain pack made up of spherical grain.

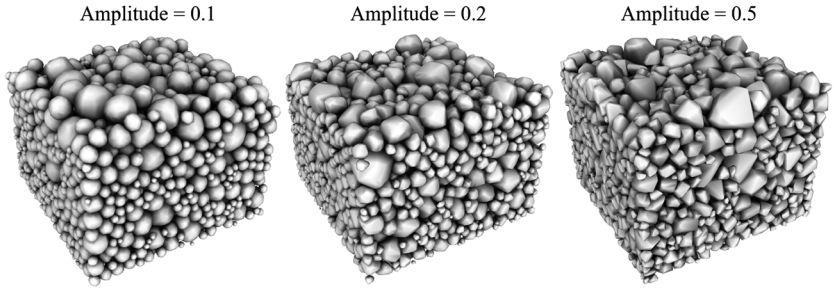

Figure 15. Random dense polydisperse grain packs of 2500 nonspherical irregularly shaped grains with Perlin noise amplitudes of 0.1, 0.2, and 0.5.

Irregularly shaped grain — Monodisperse and polydisperse grain packs

We generated 10 different random dense monodisperse grain packs with 2500 frictionless nonspherical grains (e.g., Figure 13). The shapes of the irregular grains were generated (as described in the "From spherical to nonspherical grain shapes" section) with Perlin noise amplitudes between 0 (i.e., spheres) and 1.0. The applied maximum translational and rotational shaking magnitudes are $0.0002 \times D_{\text{container}}$. All of the grains have the same properties as in the previous sections. The porosity as a function of Perlin noise amplitude is illustrated in Figure 14. The initial porosity is consistent with other studies, which typically report a porosity of approximately 0.36 (Baule and Makse, 2014). The porosity decreases as a function of Perlin noise amplitude from 0.36 to 0.28. There is a drastic porosity reduction when the Perlin noise amplitude increases from 0 to 0.2. This indicates that a little bit of surface roughness, or angularity of the grains, which is observed in most real granular media, greatly affects the expected dense packing porosity. Once the Perlin noise amplitude exceeds 0.4, the porosity does not change.

In addition to the monodisperse grain packs, we also explored polydisperse grain packs. We numerically generated 10 different random dense polydisperse grain packs of frictionless nonspherical grains with Perlin noise amplitudes between 0 and 1.0. The random dense grain packs are generated by pouring 2500 grains with a prescribed log-normal size distribution and Perlin noise amplitudes (e.g., Figure 15). The applied maximum translational and rotational shaking magnitudes are $0.0002 \times D_{\text{container}}$. All of the grains have the same properties as in previous sections. The porosity as a function of the Perlin noise amplitude is illustrated in Figure 16. The porosity of the random dense polydisperse packing of spherical grains with a Perlin noise amplitude of zero is approximately 0.32. The porosity decreases as a function of Perlin noise amplitudes from 0.32 to 0.24. Similarly to monodisperse packing, drastic porosity reduction occurs when the Perlin noise amplitude increases from 0 to 0.2. Once the Perlin noise amplitude exceeds 0.3, the porosity does not change significantly.

CONCLUSION

We introduced software for generating 3D grain packs of spherical as well as nonspherical (regular and irregular)-shaped grains with prescribed size distributions and grading. We used a DEM method to assemble grain packs with spherical and nonspherical shapes under the influence of gravitational forces. An efficient approach to creating nonspherical irregular shapes using coherent noise modification of the spherical grain surface is also presented. Various random loose and dense grain packs of spherical and nonspherical (regular and irregular) grains are presented to show the validity and consistency of the generated packs as compared with previous studies in the

literature. Results show that a small increase in the roughness of the grains results in a relatively large decrease in porosity.

Several improvements are planned. The current numerical framework is implemented using a recent version of PhysX that uses a CPU. This allows for the generation of thousands to tens of thousands of grains in a reasonable time (minutes to tens of minutes). Newer versions of PhysX using GPUs in some steps of the system, such as contact detection, will increase the efficiency drastically (5×–10× depending on the number of grains simulated) and allow for the simulation of tens of thousands of grains in seconds to tens of seconds. Finally, the current collision detection algorithm only works on convex shapes. This means that concave shapes cannot be used to generate nonspherical grains. Once automatic convex decomposition is implemented, this limitation can be overcome.

ACKNOWLEDGMENTS

We would like to thank the Stanford Rock Physics & Borehole Geophysics Project and Stanford Center for Earth Resources Forecasting for their support and valuable discussions. We also acknowledge the helpful reviews from J. Shragge and T. Poulet. Finally, we would like to thank Saudi Aramco and the dean of the School of Earth, Energy, and Environmental Sciences at Stanford University, S. Graham, for funding.

DATA AND MATERIALS AVAILABILITY

Data associated with this research are available and can be accessed via the following URL: https://github.com/StanfordRockPhysics/ParticlePack.

REFERENCES

Abou-Chakra, H., J. Baxter, and U. Tüzün, 2004, Three-dimensional grain shape descriptors for computer simulation of non-spherical particulate assemblies: Advanced Powder Technology, **15**, 63–77, doi: 10.1163/15685520460740070.

Al-Raoush, R. I., and M. Alsaleh, 2007, Simulation of random packing of polydisperse grains: Powder Technology, **176**, 47–55, doi: 10.1016/j.powtec.2007.02.007.

Anitescu, M., and F. A. Potra, 1997, Formulating dynamic multi-rigid-body contact problems with friction as solvable linear complementarity problems: Nonlinear Dynamics, **14**, 231–247, doi: 10.1023/A:1008292328909.

Aparicio, N. D., and C. F. Cocks, 1995, On the presentation of random packings of spheres for sintering simulations: Acta Metallurgica et Materialia, **43**, 3873–3884, doi: 10.1016/0956-7151(95)90170-1.

Bagi, K., 2005, An algorithm to generate random dense arrangements for discrete element simulations of granular assemblies: Granular Matter, **7**, 31–43, doi: 10.1007/s10035-004-0187-5.

Bannerman, M. N., R. Sargant, and L. Lue., 2011, DynamO: A free O(N) general event-driven molecular dynamics simulation: Journal of Computational Chemistry, **32**, 3329–3338, doi: 10.1002/jcc.v32.15.

Barber, C. B., D. P. Dobkin, and H. Huhdanpaa, 1995, The Quickhull algorithm for convex hulls: ACM Transactions on Mathematical Software, **22**, 469–483, doi: 10.1145/235815.235821.

Baule, A., and H. Makse, 2014, Fundamental challenges in packing problems: From spherical to non-spherical grains: Soft Matter, **10**, 4423–4429, doi: 10.1039/c3sm52783b.

Bernal, J. D., 1959, A geometrical approach to the structure of liquids: Nature, **183**, 141–147, doi: 10.1038/183141a0.

Camborde, F., C. Mariotti, and F. V. Donzé, 2000, Numerical study of rock and concrete behavior by discrete element modeling: Computer and Geotechnics, **27**, 225–247, doi: 10.1016/S0266-352X(00)00013-6.

Cignoni, P., M. Callieri, M. Corsini, M. Dellepiane, F. Ganovelli, and G. Ranzuglia, 2008, Meshlab: An open-source mesh processing tool: Presented at the Eurographics Italian Chapter Conference.

Cundall, P. A., and O. D. A. Strack, 1979, A discrete numerical model for granular assemblies: Géotechnique, **29**, 47–65, doi: 10.1680/geot.1979.29.1.47.

Diyokeugwu, A., and P. Glover, 2018, Grain-mixing modeling of the porosity and permeability of binary mixtures: 88th Annual International Meeting, SEG, Expanded Abstracts, 3463–3467, doi: 10.1190/segam2018-2975312.1.

Donev, A., I. Cisse, D. Sachs, E. A. Variano, F. H. Stillinger, R. Connelly, S. Torquato, and P. M. Chaikin, 2004, Improving the density of jammed disordered packings using ellipsoids: Science, **303**, 990–993, doi: 10.1126/science.1093010.

Donev, A., S. Torquato, and F. H. Stillinger, 2005a, Neighbor list collision-driven molecular dynamics simulation for nonspherical hard grains. I: Algorithmic details: Journal of Computational Physics, **202**, 737–764, doi: 10.1016/j.jcp.2004.08.014.

Donev, A., S. Torquato, and F. H. Stillinger, 2005b, Neighbor list collision-driven molecular dynamics simulation for nonspherical hard grains. II: Applications to ellipses and ellipsoids: Journal of Computational Physics, **202**, 765–793.

Donzé, F. V., V. Richefeu, and S.-A. Magnier, 2009, Advances in discrete element method applied to soil, rock and concrete mechanics: Electronic Journal of Geotechnical Engineering, **8**, 44–88.

Dullien, F. A. L., 1991, Porous media: Fluid transport and pore structure, 2nd ed.: Academic Press.

Finney, J. L., 1970, Random packings and the structure of simple liquids: I. The geometry of random close packing: Proceedings of the Royal Society of London: Series A, Mathematical and Physical Science, **319**, 479–493, doi: 10.1098/rspa.1970.0189.

Fischer, K., B. Gärtner, and M. Kutz, 2003, Fast smallest-enclosing-ball computation in high dimensions, *in* G. Di Battista and U. Zwick, eds., Algorithms-ESA 2003: Springer, Lecture Notes in Computer Science, 630–641.

Fu, G., and W. Dekelbab, 2003, 3-D random packing of polydisperse grains and concrete aggregate grading: Powder Technology, **133**, 147–155, doi: 10.1016/S0032-5910(03)00082-2.

Gao, R., X. Du, Y. Zeng, Y. Li, and J. Yan, 2012, A new method to simulate irregular grains by discrete element method: Journal of Rock Mechanics and Geotechnical Engineering, **4**, 276–281, doi: 10.3724/SP.J.1235.2012.00276.

García, X., M. Araujo, and E. Medina, 2004, P-wave velocity-porosity relations and homogeneity lengths in a realistic deposition model of sedimentary rock: Waves in Random Media, **14**, 129–142, doi: 10.1088/0959-7174/14/2/004.

García, X., J.-P. Latham, J. Xiang, and J. P. Harrison, 2009, A clustered overlapping sphere algorithm to represent real grains in discrete element modeling: Géotechnique, **59**, 779–784, doi: 10.1680/geot.8.T.037.

García, X., and E. A. Medina, 2006, Hysteresis effects studied by numerical simulations: Cyclic loading-unloading of a realistic sand model: Geophysics, **71**, no. 2, F13–F20, doi: 10.1190/1.2181309.

Gatzke, T. D., and C. M. Grimm, 2006, Estimating curvature on triangular meshes: International Journal of Shape Modeling, **12**, 1–28, doi: 10.1142/S0218654306000810.

Gavrea, B. I., M. Anitescu, and F. A. Potra, 2008, Convergence of a class of semi-implicit time-stepping schemes for non-smooth rigid multibody dynamics: SIAM Journal on Optimization, **19**, 969–1001, doi: 10.1137/060675745.

Guo, C., Y. Chen, O. Alnasery, and G. Mavko, 2018, Sensitivity of the effective electrical properties of porous rock model to the geometry of the pore space: Presented at the SEG 2018 Workshop: Reservoir Geophysics.

Hahn, J. K., 1988, Realistic animation of rigid bodies: Computer Graphics, **22**, 299–308, doi: 10.1145/378456.

Hart, R., P. A. Cundall, and J. Lemos, 1988, Formulation of a three-dimensional distinct element model. Part II: Mechanical calculations for motion and interaction of a system composed of many polyhedral blocks: International Journal of Rock Mechanics and Mining Sciences and Geomechanics Abstracts, **25**, 117–125, doi: 10.1016/0148-9062(88)92294-2.

Jerier, J.-F., V. Richefeu, D. Imbault, and V. Donzé, 2010, Packing spherical discrete elements for large scale simulations: Computer Methods in Applied Mechanics and Engineering, **199**, 1668–1676, doi: 10.1016/j.cma.2010.01.016.

Jiang, M. J., J. M. Konrad, and S. Leroueil, 2003, An efficient technique for generating homogenous specimens for DEM studies: Computer and Geotechnics, **30**, 579–597, doi: 10.1016/S0266-352X(03)00064-8.

Jin, G., T. W. Patzek, and D. B. Silin, 2003, Physics-based reconstruction of sedimentary rocks: Presented at the SPE Western Regional/AAGP Pacific Section Joint Meeting, SPE 83587.

Jodrey, W. S., and E. M. Tory, 1985, Computer simulation of close random packing of equal spheres: Physical Review A, **32**, 2347–2351, doi: 10.1103/PhysRevA.32.2347.

Jullien, R., and P. Meakin, 2000, Computer simulations of steepest descent ballistic deposition: Colloids and Surfaces A: Physicochemical and Engineering Aspects, **165**, 405–422, doi: 10.1016/S0927-7757(99)00445-8.

Kansal, A. R., S. Torquato, and F. H. Stillinger, 2002, Computer generation of dense polydisperse sphere packings: Journal of Chemical Physics, **117**, 8212–8218, doi: 10.1063/1.1511510.

Kerimov, A., G. Mavko, T. Mukerji, J. Dvorkin, and M. A. Al Ibrahim, 2018, The influence of convex particles' irregular shape and varying size

on porosity, permeability, and elastic bulk modulus of granular porous media: Insights from numerical simulations: Journal of Geophysical Research, **123**, 10,563–10,582, doi: 10.1029/2018JB016031.

Kloss, C., C. Goniva, A. Hager, S. Amberger, and S. Pirker, 2012, Models, algorithms and validation for opensource DEM, and CFD-DEM: Progress in Computational Fluid Dynamics, **12**, 140–152, doi: 10.1504/PCFD.2012.047457.

Knackstedt, M. A., S. Latham, M. Madadi, A. Sheppard, T. Varslot, and C. Arns, 2009, Digital rock physics: 3D imaging of core material and correlations to acoustic and flow properties: The Leading Edge, **28**, 28–33.

Latham, J.-P., Y. Lu, and A. Munjiza, 2001, A random method for simulating loose packs of angular grains using tetrahedral: Géotechnique, **51**, 871–879, doi: 10.1680/geot.2001.51.10.871.

Latham, J.-P., and A. Munjiza, 2004, The modeling of grain systems with real shapes: The modeling of grain systems with real shapes: Philosophical Transactions of the Royal Society A, **362**, 1953–1972, doi: 10.1098/rsta.2004.1425.

Lee, Y., C. Fang, Y.-R. Tsou, L.-S. Lu, and C.-T. Yang, 2009, A packing algorithm for three-dimensional convex grains: Granular Matter, **11**, 307–315, doi: 10.1007/s10035-009-0133-7.

Lin, X., and T.-T. Ng, 1997, A three-dimensional discrete element model using arrays of ellipsoids: Géotechnique, **47**, 319–329, doi: 10.1680/geot.1997.47.2.319.

Liu, L., and Y. Yuan, 2000, Dynamic simulation of powder compact by random packing of monosized and polydisperse grains: Journal of Material Science Letters, **19**, 841–843, doi: 10.1023/A:1006721011545.

Longshaw, S. M., 2011, Numerical modeling and visualization of the evolution of extensional fault systems: Ph.D. thesis, University of Manchester.

Longshaw, S. M., M. J. Turner, E. Flinch, and R. Gawthorpe, 2010, Analyzing the use of real-time physics engines for scientific simulation: Exploring the theoretical and practical benefits for discrete element modeling: Presented at the 18th UK Conference on Computational Mechanics.

Lubachevsky, B. D., and F. H. Stillinger, 1990, Geometric properties of random disk packings: Journal of Statistical Physics, **60**, 561–583, doi: 10.1007/BF01025983.

Magnier, S. A., and F. V. Donzé, 1998, Numerical simulations of impacts using a discrete element method: Mechanics of Cohesive-Frictional Materials, **3**, 257–276, doi: 10.1002/(SICI)1099-1484(199807)3:3<257::AID-CFM50>3.0.CO;2-Z.

Man, W., A. Donev, F. H. Stillinger, M. T. Sullivan, W. B. Russel, D. Heeger, S. Inati, S. Torquato, and P. M. Chaikin, 2005, Experiments on random packing of ellipsoids: Physical Review Letters, **94**, 198001, doi: 10.1103/PhysRevLett.94.198001.

Martin, C. L., 2004, Elasticity, fracture and yielding of cold compacted metal powders: Journal of the Mechanics and Physics of Solids, **52**, 1691–1717, doi: 10.1016/j.jmps.2004.03.004.

Martin, C. L., D. Bouvard, and S. Shima, 2003, Study of grain rearrangement during powder compaction by discrete element method: Journal of Mechanics and Physics of Solids, **51**, 667–693, doi: 10.1016/S0022-5096(02)00101-1.

Matsushima, T., H. Saomoto, M. Matsumoto, K. Toda, and Y. Yamada, 2003, Discrete element simulation of an assembly of irregularly-shaped grains: Quantitative comparison with experiments: Presented at the 16th Engineering Mechanics Conference, ASCE.

Matuttis, H.-G., and J. Chen, 2014, Understanding the discrete element method: Simulation of no-spherical grains for granular and multi-body system: Wiley.

Messmer, P., 2014, Crash, boom, bang! Leveraging game physics and graphics APIs for scientific computing: Presented at the GPU Technology Conference.

Mirtich, B. V., 1996, Impulse-based dynamic simulation of rigid body systems: Ph.D. thesis, University of California Berkeley.

Monteiro Azevedo, N., J. V. Lemos, and J. Rocha de Almeida, 2008, Influence of aggregate deformation and contact behavior on discrete grain modeling of fracture of concrete: Engineering Fracture Mechanics, **75**, 1569–1586, doi: 10.1016/j.engfracmech.2007.06.008.

Mustoe, G. G. W., and M. Miyata, 2001, Material flow analysis of non-circular-shaped granular media using discrete element methods: Journal of Engineering Mechanics, **127**, 1017–1026, doi: 10.1061/(ASCE)0733-9399(2001)127:10(1017).

Nurkanov, E. Y., R. M. Kadushnikov, I. G. Kemenin, D. M. Alievskii, and V. V. Kartashov, 2001, Theory and technology of sintering, heat, and chemical heat-treatment processes: Powder Metallurgy and Metal Ceramics, **40**, 229–235, doi: 10.1023/A:1012893113593.

O'Donovan, J., E. Ibrahim, C. O'sullivan, S. Hamlin, and M. Wood, 2016, Micromechanics of seismic wave propagation in granular materials: Granular Matter, **18**, 1–18, doi: 10.1007/s10035-015-0597-6.

Paterson, N. R., 1956, Seismic wave propagation in porous granular media: Geophysics, **21**, 691–714, doi: 10.1190/1.1438261.

Perlin, K., 1985, An image synthesizer: Presented at the SIGGRAPH '85, ACM SIGGRAPH Computer Graphics, 287–296.

Perlin, K., 2002, Improving noise: Proceedings of the 29th Annual Conference on Computer Graphics and Interactive Techniques, 681–682.

Popko, E. S., 2012, Divided spheres: Geodesics and the orderly subdivision of the sphere: CRC Press.

Pöschel, T., and T. Schwager, 2005, Computational granular dynamics: Models and algorithms: Springer.

Price, M., V. Murariu, and G. Morrison, 2007, Sphere clump generation and trajectory comparison for real grains: Presented at the Discrete Element Methods Conference.

Richefeu, V., M. S. El Youssoufi, and F. Radjai, 2006, Shear strength properties of wet granular materials: Physical Review E: Statistical, Nonlinear, and Soft Matter Physics, **73**, 051304, doi: 10.1103/PhysRevE.73.051304.

Sain, R., 2010, Numerical simulation of pore-scale heterogeneity and its effects on elastic, electrical and transport properties: Ph.D. thesis, Stanford University.

Sain, R., T. Mukerji, and G. Mavko, 2014, How computational rock-physics tools can be used to simulate geologic processes, understand pore-scale heterogeneity, and refine theoretical models: The Leading Edge, **33**, 324–334, doi: 10.1190/tle33030324.1.

Sain, R., T. Mukerji, and G. Mavko, 2016, On microscale heterogeneity in granular media and its impact on elastic property estimation: Geophysics, **81**, no. 6, D561–D571, doi: 10.1190/geo2016-0152.1.

Scott, G. D., 1962, Radial distribution of the random close packing of equal spheres: Nature, **194**, 956–957, doi: 10.1038/194956a0.

Stillinger, F. H., and B. D. Lubachevsky, 1993, Crystalline-amorphous interface packings for disks and spheres: Journal of Statistical Physics, **73**, 497–514, doi: 10.1007/BF01054337.

Storey, K., 2017, Game physics on the GPU with PhysX 3.4: Presented at the Game Developer Conference.

Storey, K., M. Lu, S. Schirm, and B. Galdrikian, 2018, NVidia physics: New simulation features: Presented at the Game Developer Conference.

Tahmasebi, P., 2018, Packing of discrete and irregular particles: Computers and Geotechnics, **100**, 52–61, doi: 10.1016/j.compgeo.2018.03.011.

Tahmasebi, P., and M. Sahimi, 2018, A stochastic multiscale algorithm for modeling complex granular materials: Granular Matter, **20**, 45, doi: 10.1007/s10035-018-0816-z.

Tahmasebi, P., M. Sahimi, and J. E. Andrade, 2017, Image-based modeling of granular porous media: Geophysical Research Letters, **44**, 4738–4746, doi: 10.1002/2017GL073938.

Tan, Y., Y. Dongmin, and Y. Sheng, 2009, Discrete element method (DEM) modeling of fracture and damage in the machining process of polycrystalline SiC: Journal of European Ceramic Society, **29**, 1029–1037, doi: 10.1016/j.jeurceramsoc.2008.07.060.

Tasora, A., and D. Negrut, 2016, A parallel algorithm for solving complex multibody problems with stream processors: International Journal of Computational Vision and Biomechanics, **2**, 131–143.

Tasora, A., D. Negrut, and M. Anitescu, 2008, A GPU-based implementation of a cone convex complementary approach for simulating rigid body dynamics with frictional contact: Presented at the International Mechanical Engineering Congress and Exposition.

Terdiman, P., 2001, Memory-optimized bounding-volume hierarchies, http://www.codercorner.com/Opcode.pdf, accessed 23 April 2017.

Tonge, R., 2012, Solving rigid body contacts: Presented at the Game Developers Conference.

Tonge, R., F. Benevolenski, and A. Voroshilov, 2012, Mass splitting for jitter-free parallel rigid body simulation: ACM Transactions on Graphics, **31**, 1–8, doi: 10.1145/2185520.

Unity Technologies, 2017, Unity 2017.1.0b8, www.unity3d.com, accessed 10 June 2017.

Wadell, H., 1935, Volume, shape and roundness of quartz grains: The Journal of Geology, **43**, 250–280, doi: 10.1086/624298.

Wang, L., J.-Y. Park, and Y. Fu, 2007, Representation of real grains for DEM simulation using X-ray tomography: Construction and Building Materials, **21**, 338–346, doi: 10.1016/j.conbuildmat.2005.08.013.

Yang, R. Y., R. P. Zou, and A. B. Yu, 2000, Computer simulation of the packing of fine grains: Physical Review E: Statistical, Nonlinear, and Soft Matter Physics, **62**, 3900–3908, doi: 10.1103/PhysRevE.62.3900.

Yin, H, and A. Nur, 1993, Porosity, permeability, and acoustic velocity in granular materials: 63rd Annual International Meeting, SEG, Expanded Abstracts, 775–778, doi: 10.1190/1.1822615.

Zhao, S., X. Zhou, W. Liu, and C. Lai, 2015, Random packing of tetrahedral grains using the polyhedral discrete element method: Particuology, **23**, 109–117, doi: 10.1016/j.partic.2015.02.007.